ISSN 2347-3487
Volume 13 Number 1
Journal of Advances in Physics

Preparation and Characterization of Silver and Gold Nanoparticles and Study Influence on Physical Properties of PVA/PVP nanocomposites

[1]Mahrous. S. Meikhail, [2]*A. M. Abdelghany, [1, 3] A. A. ALdhabi
[1] Physics Dept., Faculty of Science, Mansoura University, Mansoura, Egypt
[2] Spectroscopy Dept., Physics Division, National Research Center, 33 Elbehouth St., Cairo, 12311, Egypt
[3] Physic Department, Faculty of Science, Amran University, Yemen
* E-mail: a.m_abdelghany@yahoo.com

ABSTRACT

Gold nanoparticles (Au NPs) and Silver nanoparticles (Ag NPs) ware prepared by “green” synthesis extraction using the Chenopodium murale leaf extract, the obtained (Ag NPs and Au NPs) were investigated by UV/Vis. absorption spectroscopy, transmission electron microscopy, Zetasizer, XRD. The plant extraction leads to produce nanoparticles of spherical shape with size range from 4 to 22 nm.

Polyvinyl alcohol (PVA) and polyvinyl Pyrolidone (PVP) blend with mixed silver and gold nanoparticles were prepared by casting method. Amorphous feather of doping polymers blend was characterized by X-ray diffraction. Significant changes within the polymer matrix were monitored from infrared spectroscopy which indicates the interaction between polymer blend and mixed nanoparticles. Both indirect and direct optical energy gaps are calculated and discussed.

Keywords

Silver nanoparticles; gold nanoparticles; X-ray diffraction; transmission electron microscopy.

1- INTRODUCTION

Nanoparticles of metal have good physical and chemical properties which make them important for applications such as electronics, catalysis, optics, biotechnology and [1]. Polyvinyl alcohol (PVA) has structures of many interactions, which may be considered semicrystalline or amorphous [2]. Poly (N-vinylpyrrolidone) (PVP) deserve of polymer conjugated due to its good stability of environmental, electrical conductivity, easy processability and charge transport mechanism [3]. PVA/PVP interaction has been described in many papers due to their good properties. Nanoparticles of metal have good physical and chemical properties which make them important for application in the fields of nanotechnology and biotechnology. In this respect, silver nanoparticles (Ag NPs) and gold nanoparticles (Au NPs) have drawn attention of many researches in the past few years, because of their suitable application in the fields of electronics, material science and medicine [4]. Gold nanoparticles (Au NPs) are of increasing interest in chemistry of materials because the broad versatility of chemical of the gold nanoparticles themselves and resulting colloidal matrix [5]. Gold nanoparticles have been used in nanotechnology and biotechnology because their optical properties in the visible spectrum and high bio affinity. Polymer metal nano composites samples are crossbred materials with different inorganic nanoparticles in polymer matrix. Metal nanoparticles such as silver (Ag) and gold (Au) contributes in their characteristic optical [5]. Where used to the biosynthesis of gold or silver nanoparticles using plant of (Chenopodium murale) extract. In this study, we described a novel method for preparation of PVA/PVP polymer matrix containing a mixed Ag and Au nanoparticles.

2. MATERIALS AND EXPERIMENTAL WORK

2.1. Materials

The polyvinyl alcohol from Merck, Germany has molecular weight 14,000 and the polyvinyl pyrrolidone molecular weight 40000 from Aldrich Chemical Co. Ltd., were used as a basic polymeric materials. The tetrachloroauric (III) acid trihydrate ($HAuCl_4$-$3H_2O$, 99.5% GR of analysis) was obtained from Merk, Germany. The Silver nitrate ($AgNO_3$) was obtained from Sigma–Aldrich chemicals. The water deionized was used during the reactions as solvent. The quantity was equal of PVA and PVP (50/50) by weight was added to doubly distilled water with stirring the solution at room temperture to complete dissolution. The nanoparticles was dissolved in doubly distilled water and added to the solution of polymeric matrix with continuous stirring. The solution was poured onto cleaned Petri dishes and dried in oven at 50 ^{0}C for 5 days to ensure removal of the solvent traceses. The films were peeled from Petri dishes, After drying and kept in vacuum desiccators until use. The thickness of the samples was in the range of 0.1 – 0.3 mm.

Table 1. Required amount of Ag , Au and mixed Nanoparticles empedded within polymer blend

Sample	Ag NPs (ml)	Au NPs (ml)	(Ag-Au) NPs %	NPs Wt. %
Pure	0	0	0	0
$Ag_{100}Au_0$	4	0	100 – 0	0.15
$Ag_{75}Au_{25}$	3	1	75 – 25	0.15
$Ag_{50}Au_{50}$	2	2	50 – 50	0.15
$Ag_{25}Au_{75}$	1	3	25 – 75	0.15
Ag_0Au_{100}	0	4	0 – 100	0.15

2.2. Preparation of Chenopodium Murale Extract

The leaves of Chenopodium murale was collected from Egyptian farms. Fresh leaf extract, used for the biosynthesis of Ag NPs and Au NPs, was prepared from 15 g of Chenopodium murale completely washed in 400 ml Erlenmeyer flask, boiled in 60 ml distilled water for about 1hr. The extract produced was preserved to the freeze drying. The obtained filtrate was filtered using Whatman No. 40 paper filters [6, 7].

2.3. Preparation of Gold and Silver Nanoparticles Using Extract of (C. murale)

4 ml of the extract (Chenopodium murale) was added to 100 ml 4 mM gold chloride ($HAuCl_4$. $3H_2o$) solutions at room temperature. Change of the color was observed after 24 hr in the dark from yellow to violet color that indicate formation of Au NPs in solution stored at 4°C. Chenopodium murale extract (4-6) ml was added to 100 ml 2.3 mM $AgNO_3$ solution and the volume was modulated with deionized water. Reduction process of Ag^+ to Ag^0 nanoparticles was observed by the change of color from transparent white to the ruby red after 24 hr indicate the presence of silver nanoparticles.

2.4. Characterization Techniques

The X-ray diffraction (XRD) scans were performed using PANalytical X`Pert PRO X-ray diffraction system using Cu Kα radiation, tube operated at 30 kV, Bragg's angle (2θ) from range 4-80 degree. Fourier transforms infrared was recorded using single beam spectrometer (Nicolet iS10, USA) in the spectral range (4000–400) cm^{-1}. UV/Vis. were measured in the wavelength range 190-900 nm by (V-570 UV/VIS/NIR, JASCO, and Japan) double beam spectrophotometer to investigated structural changes result from addition of the mixed nanoparticles and to retrace changes in their optical properties. Particle size distribution and the shape was investigated by JEOL JEM 2100 Japan (TEM) "Transmission Electron Microscope" worked at accelerated voltage of 160 kV. The surface charge of the gold nanoparticles in various solutions was measured by using a zeta potential analyzer by used Zetasizer APS Essentials manual UV Instruments Ltd. Enigma Business Park, Grovewood Road, MAN0426-1.0/ MAN0429-1.0 United Kingdom. Silver and gold concentrations measurements were studied via atomic absorption, where silver and gold concentrations were found to be 380 and 460 ppm respectively.

3. RESULTS AND DISCUSSIONS

3.1. UV-Vis. Optical Studies for (Ag NPs/Au NPs) and Mixed Nanoparticles

Fig. 1 show of the UV/Vis. spectrum in the range of 190-800 nm and shows characteristic broad band of the formation Ag NPs and exhibits a peak at 424 nm this absorption related to the Surface Plasmon Resonance (SPR) of silver nanoparticles (Ag NPs) [8, 9, 10]. Fig. 2 show's broad band at about 536 nm this peak corresponding to Surface Plasmon Resonance for the prepared of gold NPs [11, 12, 13]. UV-Vis absorption spectra of mixed nanoparticles was shown in fig 3. The optical spectra shows a two absorptions peaks at 228 nm and 350 nm that assigned to the presence of trace amount of iron impurities in plant extract [14]. The band of absorption was appeared at 536 nm related to the surface plasmon resonance of Au NPs [12, 7, 15, 16]. The absorption band at 424 nm assigned to surface plasmon resonance for Ag NPs [10, 17, 18, 19, 20]. When the gold or silver nanoparticles, smaller than 5 nm, are hard to distinguish and yield broad peaks as their SPR bands. Mixing of silver and gold result in a shift and/or overlap of bands of SPR band acompined with a decreases in intensity of the broad band indicating the formation of spherical shape and homogeneous distribution of silver and gold nanoparticles [3, 20]. Shifting of the SPR band result from increasing of the mole fractions of gold nanoparticles. This phenoimena indicates an interaction between silver-gold and formation of a core-shell nanoparticles as indicated previously [21]. UV-Vis. spectra of mixed nanoparticles was shows a weak and broad band point out for the formation of a non monodispersed nano particles assemblies is still a significantly challenge towards the actual applications of nanostructured system [22]. The intensity of broad band (SPR) was decreases with increasing volume of Au NPS from 25% to 75% Au NPs. This indicate the plasmon peak is mainly corresponding to the small size distribution of the prepared gold nanoparticles and dependent on the number of the reduced silver nanoparticles [23, 24].

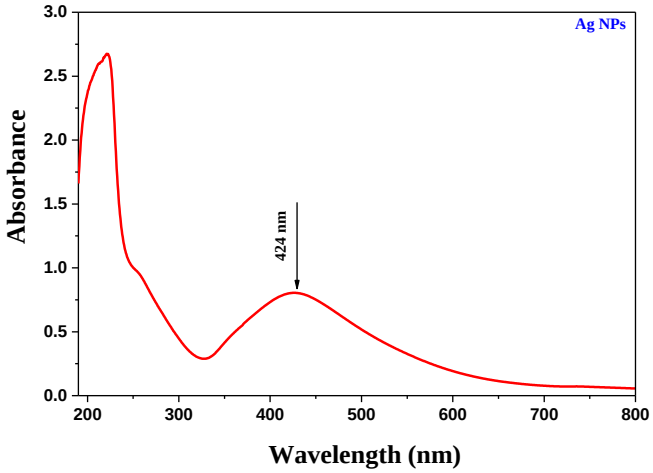

Fig. 1. UV/Vis. spectra for silver nanoparticles SPR

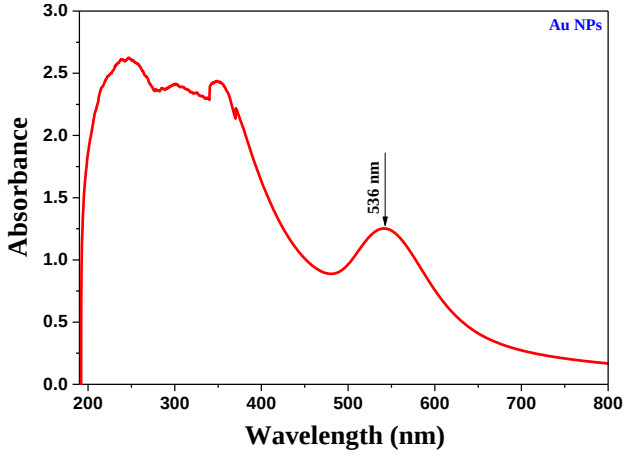

Fig. 2. UV/Vis. spectra for gold nanoparticles SPR

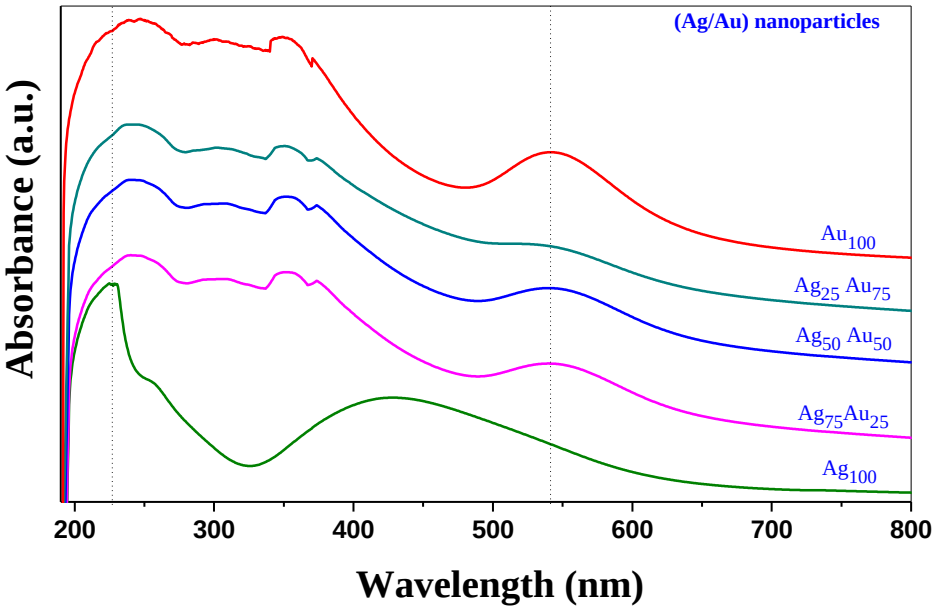

Fig. 3. The spectra of UV-Vis. Ag NPs and Au NPs and mixed nanoparticles

3.2. Transmission Electron Microscopy

The images of transmission electron microscopy were used to determine of the particle size, size distribution and shape of the nanoparticles. Imaging direct gives a fast automated image to analysis solution. Fig. 4, fig. 5 shows transmission electron microscopy images of the silver and gold nanoparticles prepared respectively and size distribution of well-dispersed suspension, the size of silver and gold nanoparticles has been determined by measuring the diameter of whole particles. We can see that the nanoparticles are mainly spherical and different size of silver and gold nanoparticles and are distribution of semi regularly. From fig.4 it can see that silver nanoparticles are mainly spherical shape and different size where the average size was 12 nm and dispersed homogeneously. Fig. 5 shows transmission electron microscopy (TEM) images for Au NPs was prepared the shape are spherical with different size nanoparticle, where the average of Au NPs size of was 10 nm. Fig. 6 shows the electro diffraction of Ag and Au nanoparticle respectively, from figures we noticed that the structures of nanoparticles prepared have polycrystalline structure. Fig. 7 and Fig. 8 show Zetasizer for the silver and gold nanoparticles respectively which indicates the non monodispersed state; this is because of negatively charged layer. This non monodispersity accounts for the probe preparation and generation of color signal in chromatographic strip assay.

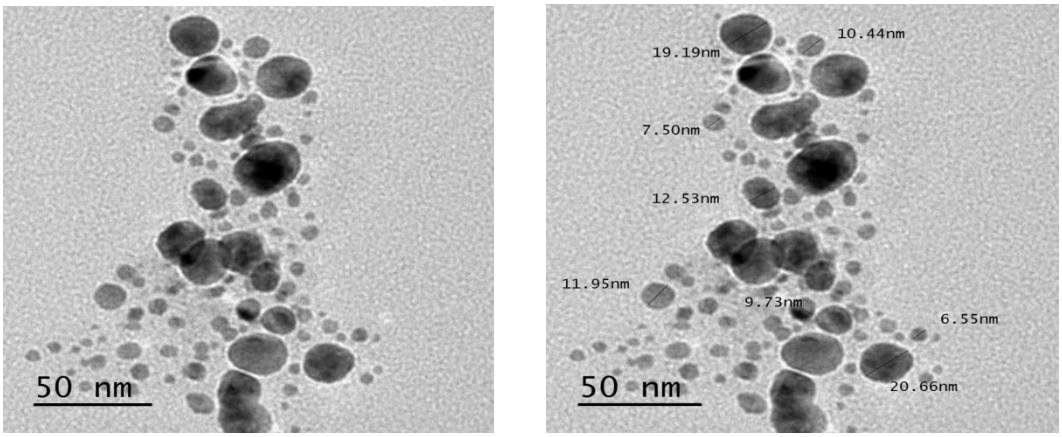

Fig. 4. TEM image of silver nanoparticles

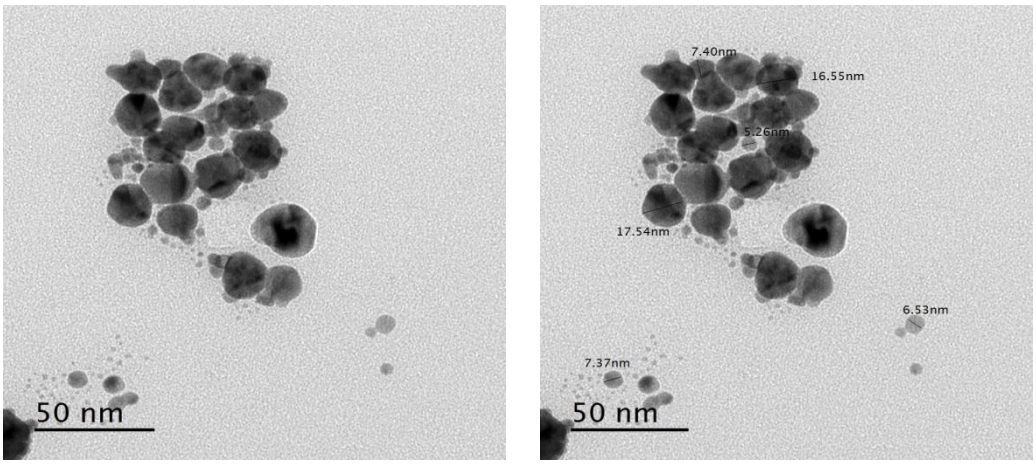

Fig. 5. TEM image of Au nanoparticles

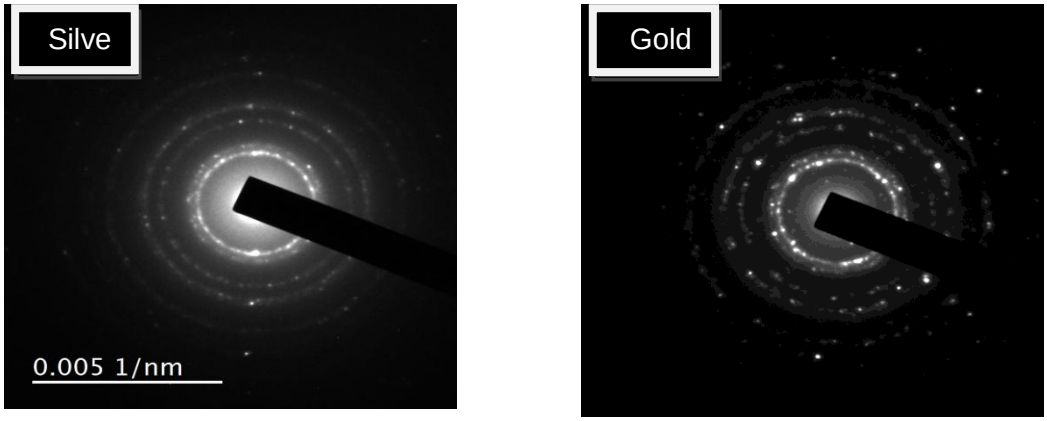

Fig. 6. Electron diffractions pattern

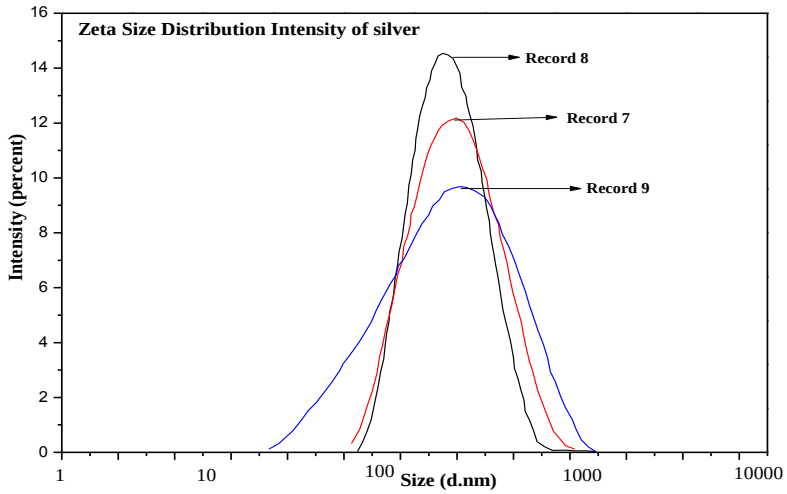

Fig. 7. Zeta Size of Ag NPs

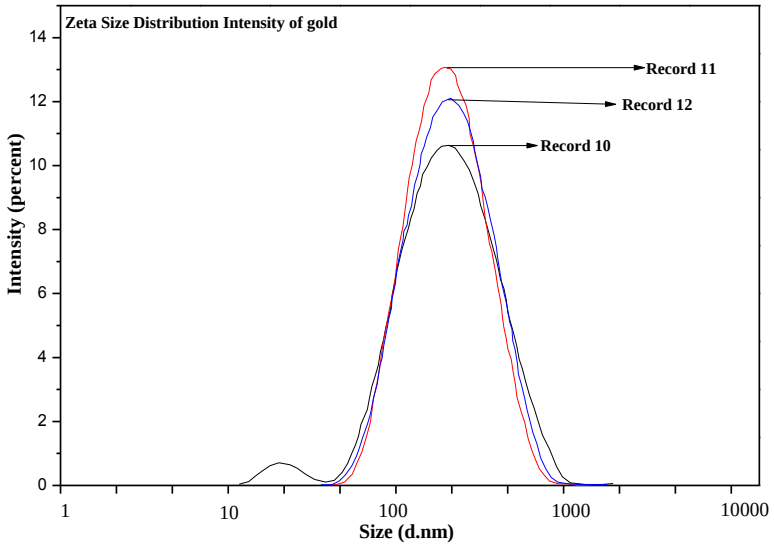

Fig. 8. Zeta Size of Au NPs

3.3. Zeta Potential Studies

The zeta-potential analyzer was used to measure the surface potential on the particle. The electrostatic potential on the surface for particles called the zeta potential. In measurement was measured the electrophoretic mobility of Ag NPs

and Au NPs based on the dynamic light scattering. The zeta study was conducted for particle size, size distribution as well as for zeta potential measurement of both bare and antibody conjugated Ag and Au nanoparticles. In the studies of used transmission electron microscopy, images show particles with lower and higher size range. The supernatant was collected and characterized for further use. For zeta potential distribution study, peak number and peak area gives important explanation. Three cycles of different counts were run and average of the counts was taken. The mean peak gives the diameter of the particles and peak area gives the percentage of mean diameter depending on the intensity. The graphs were plotted using the means of all peaks mean diameter and the intensity of peak area as shown in the Fig. 10 and Fig. 11 the zeta potential measurement is also important for characterization. The negative charge on nanoparticles due to citrate ions is another important indicator for particle size. The negative charge indicates that the particle size is smaller than 100 nm [25]. In present study, zeta potential of the synthesized nanoparticles was negative. Nanoparticles synthesized by this method were very good for preparation of the stability.

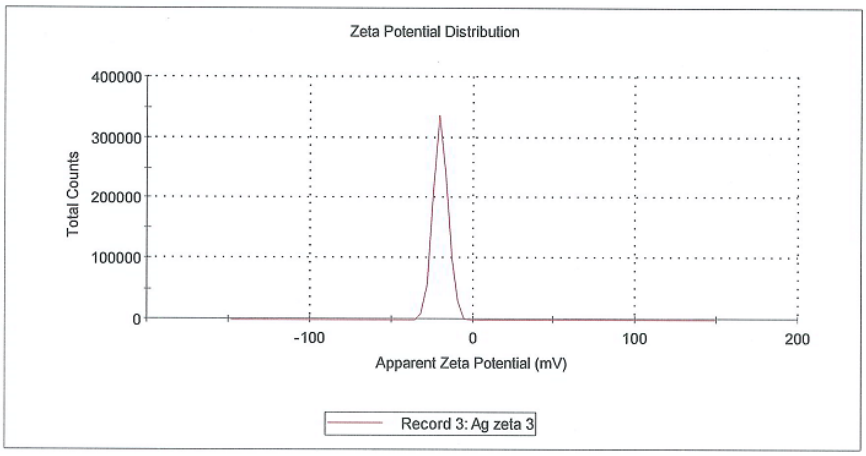

Fig. 9. The Zeta Potential of Silver nanoparticles

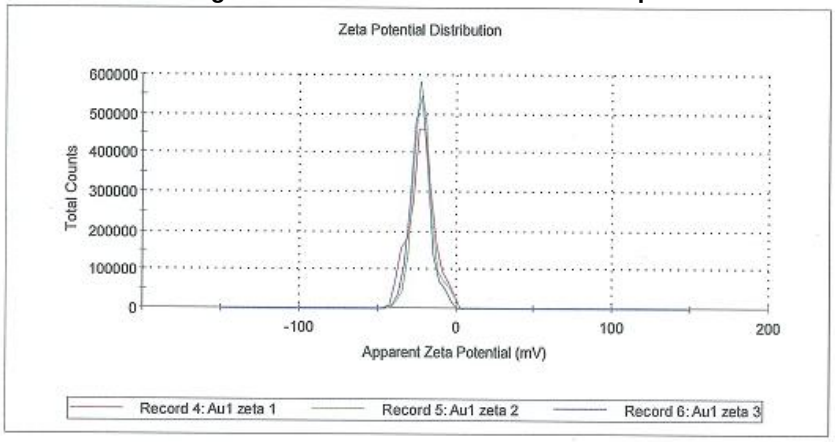

Fig. 10. The Zeta Potential of Gold nanoparticles

3.4. Fourier Transform Infrared Analysis

FT-IR spectroscopy is especially well suitable for analysis of materials that can Identify on the functional groups which including esters, amides, carboxylic acids, alcohols, carbohydrates and proteins. The technique FT-IR spectroscopy it is very powerful technique to detect the intermolecular interactions between the polymer blend and interaction with nanoparticles (Ag NPs/Au NPs). The spectra of absorption FT-IR to this work were recorded at room temperatures in range 4000-400 cm^{-1}. Fig. 11 shows the absorption spectra FT-IR of PVP, PVA and PVA/PVP blend, which this indicates the homogeneity and complexion between two polymers. Fig. 12 shows the spectra of blend with different concentrations of mixed nanoparticles (Ag NPs/Au NPs). From Fig. 11, the strong and broad band at 3335 cm^{-1} is related vibration to O—H stretching of hydroxyl group [2, 26, 27]. The band at about 2926 cm^{-1} corresponding to (CH_2) methylene group, asymmetric stretching vibration [27, 28]. Appearance a sharp band of absorption at 1665 cm^{-1} assigned to C=O stretching was observed [10, 26, 27, 29, 30]. Also the appeared band at 1441 cm^{-1} that has been assigned to C=C pyridine ring [27, 31]. Absorption peak at 1292 cm^{-1} was appeared in the vibrational spectrum and its intensity was change with addition of (Ag NPs/Au NPs) this peak can be assigned to the C–N vibration stretching [10]. Appearance absorption band at 1091 cm^{-1} related to C—O stretching of acetyl groups present on backbone of PVA [27]. The band absorption at about 850 cm^{-1} is assigned to the CH_2 rocking [31]. And occurs change in intensity and shift of peaks this may indicate interaction between the (Ag NPs/Au NPs) nanoparticles of additions and the polymer blend PVA/PVP matrix and also may be because change in the crystallinity because adding of the Ag NPs and Au NPs to polymer matrix.

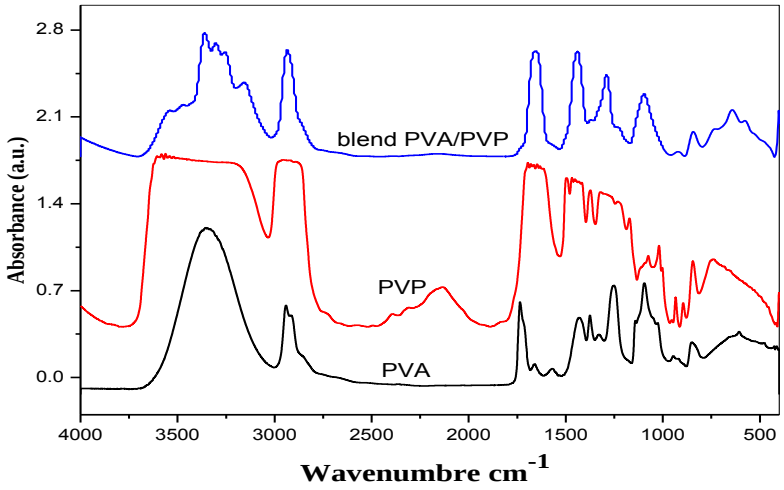

Fig. 10. FT-IR of PVA and PVP and PVA/PVP blend

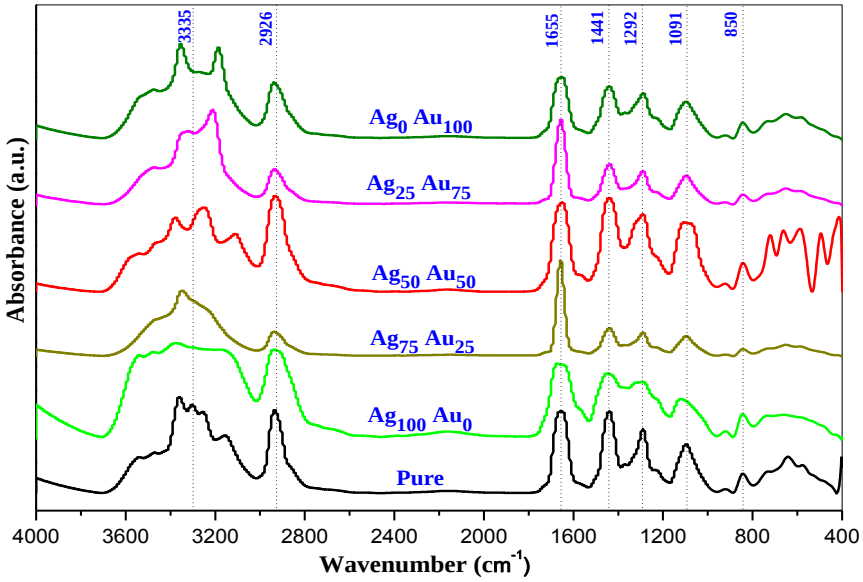

Fig. 11. The FT-IR of PVA/PVP blend and blend doped of different content of Ag and Au nanoparticles

Table 2. The bands of absorption FT-IR positions and assignment of the nanocomposite prepared films

Vibrational (cm^{-1})	Band assignment	References
3335	O–H stretching	2, 26, 27
2926	CH_2 asymmetric stretching	27, 28
1665	C=O stretching	10, 26, 27, 29, 30
1441	C=C stretching	27, 31
1292	C–N stretching	10
1091	C–O stretching	27
850	CH_2 rocking	31

3.5. Ultraviolet and Visible Analysis for PVA/PVP Doping Mixed Nanoparticles

Fig. 13 show of the UV/Vis spectra for the prepared samples, the spectra was exhibit main absorption edge for all samples at 233 nm and that shifted towards longer wavelength with increasing the (Ag NPs/Au NPs) matrix. the shift in the edge indicate the interactions between mixed nanoparticles and PVA/PVP blend and the miscibility also may be attributed between them and occur change in the crystallinity because adding of Ag and Au nanoparticles [11]. Absorption edge at about 233 nm are assigned to localized $\pi \rightarrow \pi^*$ transitions, this transition was corresponding to carbonyl groups (C=O) related with the ethylene unsaturation bond (C=C). When mixed (Ag NPs/Au NPs) is doped in PVA/PVP blend, optical properties resulting from of the electronic transitions of the two materials. The dramatic enhancement in the absorption are found to be in covenant with color change for the PVA/PVP films and transparent for the main films to ruby red of the films nanocomposites that contain of silver nanoparticles and violet color for the Au nanocomposite. The spectrum of the PVA/PVP/ and silver nanoparticles 100% nanocomposites show that the broad absorption band in visible region at 420 nm. This band is corresponding as Surface Plasmon Resonance for small amount of Ag nanoparticles and is responsible for the change colors of the films [10]. In the visible region appear the broad absorption band at about 536 nm which related as the Surface Plasmon Resonance of gold nanoparticles and is responsible of the color of the films. Reduction of silver and gold of different percentages existent in the films of the PVA/PVP blend was routinely observed by the visual inspection of the prepared films as the spectra of UV–Vis. All the films which containing the mixed nanoparticles (Ag NPs/Au NPs) in polymeric matrix. After that, the color of polymeric samples change from the transparent to ruby red of Ag and violet of Au and mild for samples contain mixed nanoparticles. The color of samples is concentrated on the percentages of nanoparticles.

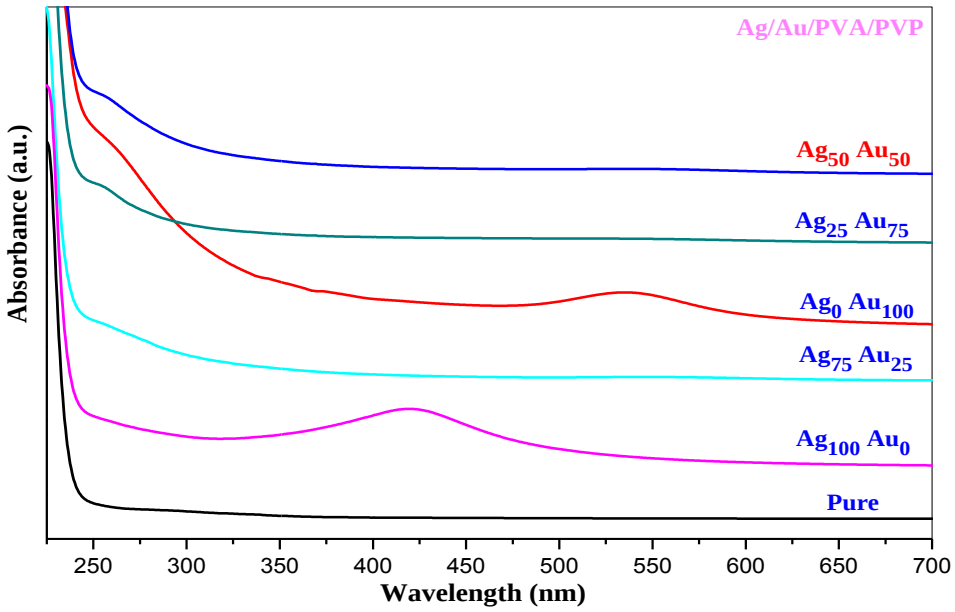

Fig. 13. Spectra of UV/Vis. of PVA/PVP pure blend and blend doped of Ag NPs and Au NPs and mixed nanoparticles

3.5.1 Study and Determination of Optical Energy gap (E_g)

The band structure can study by the optical energy absorption, in process of the absorptions an electron transitions from the lower to higher energy state. This process by absorbing a photon of known energy. There are type's possible electron transitions the fundamental absorption refers to band to band or the exciting transition. Study of the absorption and transition of electron and can be used to determine the optical band gap by ($E_g = h\ c/\lambda$). Where the absorptions is expressed in terms of a coefficient (α). Based on the Thutpalli and Tomlin [32] can be analysis the energy band gap:

$$(n\alpha h\upsilon)^2 = C_1(h\upsilon - E_{gd}) \quad (1)$$

$$(n\alpha h\upsilon)^{\frac{1}{2}} = C_2(h\upsilon - E_{gi}) \quad (2)$$

where, $h\upsilon$ is the energy of photon, E_{gi} , the indirect and E_{gd} , the direct band gap, n is a integer, C_1 , C_2 constants and α is the coefficient of absorption. Coefficient of absorption (α) can be calculated as a function of frequency by the formula:

$$\alpha(\upsilon) = 2.303 \times \frac{A}{d} \quad (3)$$

Where, d is thickness of the films under investigation and A is the absorbance.

According the Davis and Shalliday [33] the direct transition and indirect transition can occur. Can be observed the indirect transition by plotting $(\alpha h\upsilon)^{1/2}$ versus $h\upsilon$, can be observed and determine values of the energy band gap by plotting $(\alpha h\upsilon)^2$ versus $h\upsilon$, where the $h\upsilon$ is the photon energy and h is the Plank constant. The values of the band gap in this study are given in fig. 14, from the figure it is clear that the direct and indirect band gap values were decreases with increases the (Ag NPs/Au NPs) concentrations. Decreasing in the values of optical band gap indicated the presence of charge transfer complexes arose between the PVA/PVP polymer blend and mixed nanoparticles. We noticed occur the largest decrease in value band gap energies at 50% of (Ag NPs/Au NPs) in polymer blend, this may be due to the Ag act as seeds in host polymer. This results are supported by XRD and RTIR data in the present study.

3.5.2 Determination of Optical Energy Gap (E_g) using the Tauc's Expression (E_g^T)

There are other method to determine of the optical energy gap, this method it is called Tauc's expression (E_g^T) [34], the optical band gap E_g by Tauc's was used equation:

$$E_g = hc/\lambda_g \quad (4)$$

Where the c is velocity of light and h is Plank constant. By Tauc's can determines of the wavelength λ_g with plotting of the $(A^{1/2}/\lambda)$ versus $(1/\lambda)$, where A is the optical absorbance and λ is the wavelength. The optical energy gap was decrease with increase nanoparticles content within of polymer matrix and coincidence with the values of optical indirect band gap which for Davis and Mott formula. This results suggest that the indirect transition mechanism dominant one in this case.

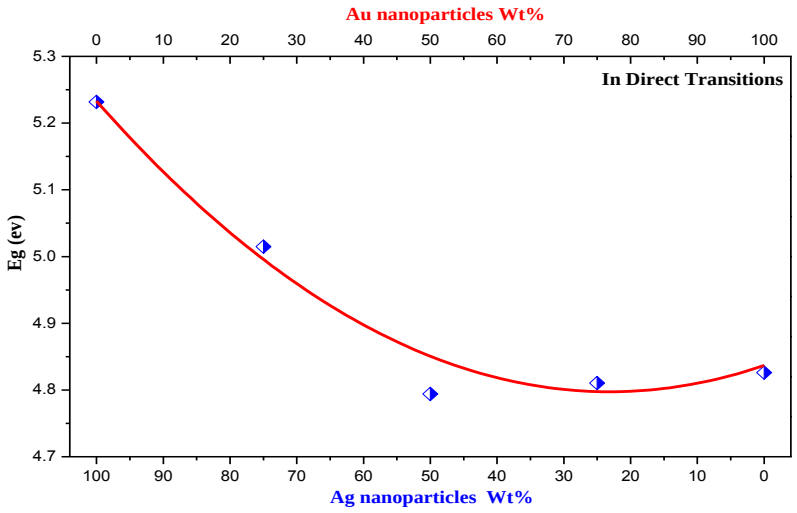

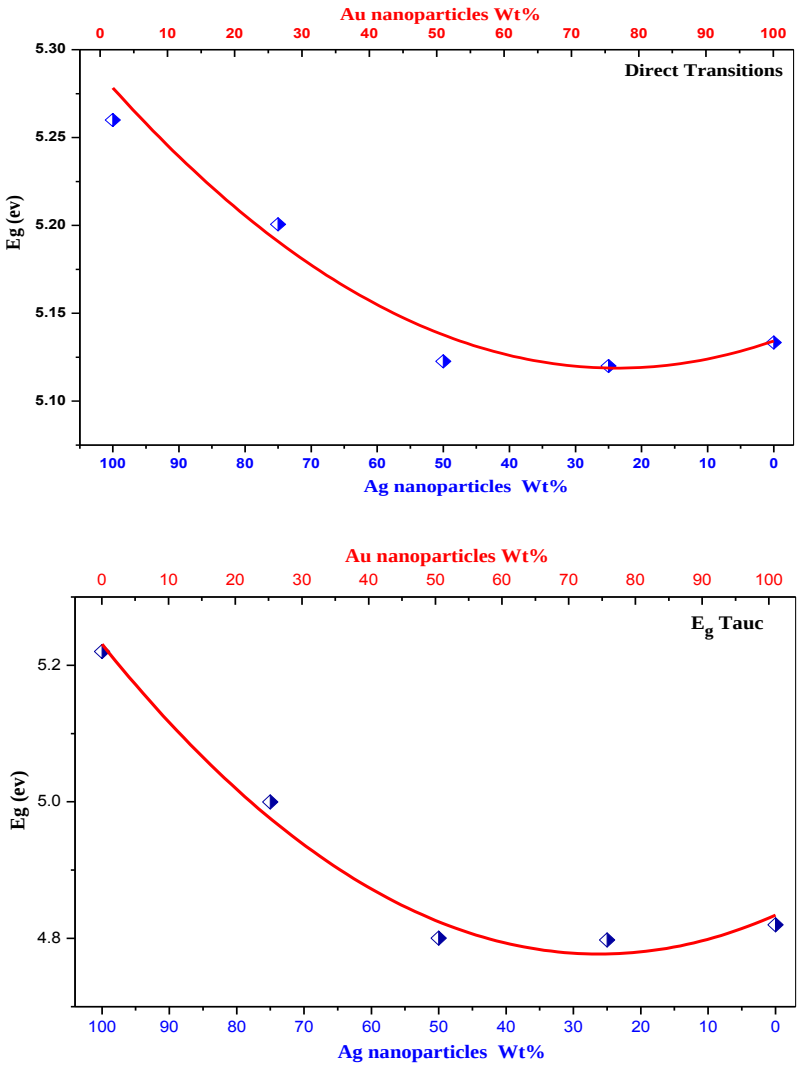

Fig. 14. The relation between E_g (eV) with content of Ag NPs / Au NPs

3.6. X-ray Diffraction Analysis (XRD)

The XRD is very important tool to investigate the structure of a polymeric materials and it enable to study of the type of structure a material is crystalline or amorphous. The PVA/PVP films and the films contain of (Ag NPs/Au NPs) was investigated by XRD. We recorded the XRD pattern broad and strong diffraction peak at $2\theta = 19.20^{o}$, this diffraction peak corresponds to (110) reflection crystallites [10]. Which are shown in fig.15 the distinguish diffraction peak of PVA/PVP blend at $2\theta = 19.20^{o}$ was observed [35, 36]. The spectra shows an amorphous feature which is distinguish by broad band for polymer blend contain different percentage of mixed nanoparticles (Ag NPs/Au NPs). The diffraction peak $2\theta = 19.20^{o}$ was occur small shift to higher angels and become to more broader (i.e. decreases of the intensity of diffraction peak) with increased of (Ag NPs/Au NPs) content. Decreasing in the intensity of this diffraction peak is an indication of decreasing crystallinity of the PVA/PVP blend because of metal incorporation. This reveals the structure of the polymer blend that contain crystalline and amorphous structure. Moreover, there are no new peaks appeared for (Ag NPs/Au NPs) indicating occur complete dissolution of nanoparticles in amorphous region of the polymeric matrix. It can be seen that, the area under the peak (A_T) and peak intensity was decreased with increasing mixed nanoparticles as fig.16. where shows that the increase in the conductivity consequently increasing in the amorphous regions within polymer matrix, this may be indicated occur interaction between polymer blend (PVA/PVP) and nanoparticles (Ag NPs /Au NPs) by the intermolecular hydrogen bonding was occurred. This means that the mixed nanoparticles was influence on the crystallinity and produce more defects in the polymer blend [22].

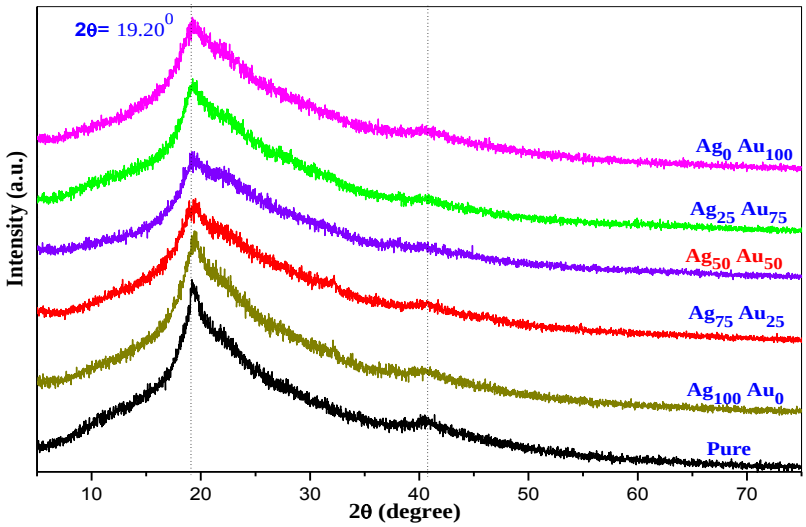

Fig. 15. XRD scans of PVA/PVP blend and blend doped with different content of Ag NPs/Au NPs.

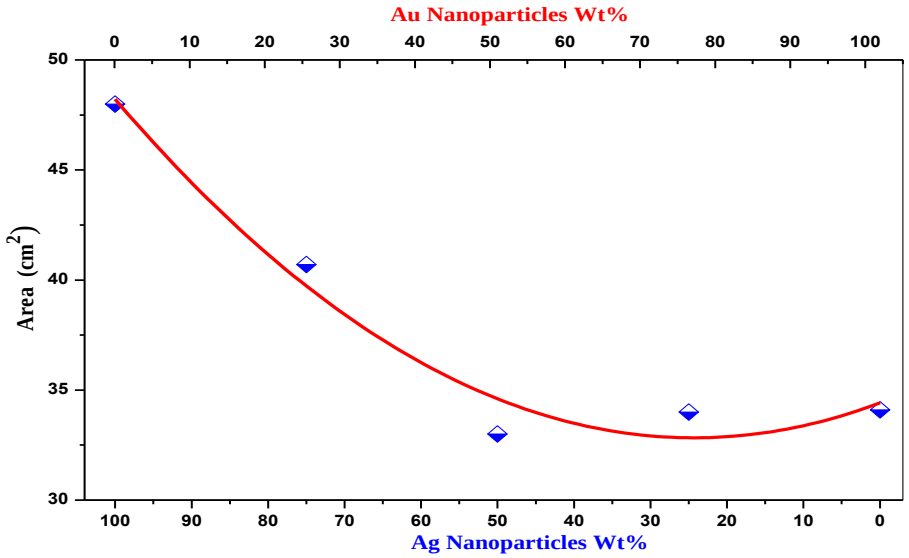

Fig. 16. Relation between Ag NPs/Au NPs concentration versus peek area

4. CONCLUSIONS

A successful method to produce Ag NPs/Au NPs, based on the Chenopodium murale by green synthesis as biosynthesize reducing for the eco-friendly synthesis. Successfully synthesized of silver (Ag) and gold (Au) nanoparticles and may be Ag act as seeds-growth route of the gold nanoparticles. Presence of the SPR at 536 nm for gold and at 424 nm at silver indicated formation of nanoparticles. TEM images for both Ag and Au shows small size and spherical shape and non monodispersed. The results of UV–visible spectra absorption and FTIR and XRD and TEM indicated that the Ag and Au nanoparticles were homogeneously dispersed in the PVA/PVP blend with narrow particle size distribution. The small size and narrow particle size distributions are obtained. Preparation of the PVA/PVP/(Ag NPs/Au NPs) nanocomposite samples in the phase solid at the room temperature. Preparation of Ag and Au nanoparticles shows that the excellent compatibility and are well dispersed in the polymer blend.

REFERENCES

[1] I. Hussain, M. Brust, A. J. Papworth, and A. I. Cooper, (2003) Langmuir. 19, 4831–4835.

[2] I. S.Elashmawi andH.E.Abdel Baieth,(2012) Curr. Appl. Phys.12,141–146.

[3] M. Alsawafta, S. Badilescu, A. Paneri, V.-V. Truong, and M. Packirisamy, (2011) Polymers (Basel). 3, 1833–1848.

[4] S. Iravani and B. Zolfaghari, (2013) Phys. Status Solidi. 9.

[5] J. D. S. Newman and G. J. Blanchard, (2007) J. Nanoparticle Res. 9, 861–868.

[6] M. A. A.-W. M.S. Abdel-Aziz, M.S. Shaheen, A.A. El-Nekeety, (2014) Saudi Chem. Soc. 18, 356–363.

[7] A. M. Abdelghany, E. M. Abdelrazek, S. I. Badr, M. S. Abdel-Aziz, and M. a. Morsi, (2015) J. Saudi Chem. Soc. 3, 277-293.

[8] E. Kirubha and P. K. Palanisamy, (2014) Adv. Nat. Sci. Nanosci. Nanotechnol. 5, 45-60.

[9] N. H. Muhammad Ahad Ahmed, (2014) ISRN Nanotechnol. 7, 14-20.

[10] W. H. Eisa, Y. K. Abdel-Moneam, a. a. Shabaka, and A. E. M. Hosam, (2012) Spectrochim. Acta Part A Mol. Biomol. Spectrosc. 95, 341–346.

[11] B. Kang and J. W. Wu, (2006). 49, 955–958.

[12] C. Sun, R. Qu, C. Ji, Y. Meng, C. Wang, Y. Sun, and L. Qi, (2009) J. Nanoparticle Res. 11, 1005–1010.

[13] D. E. J. . Pedersen D.B., (2005) Surf. Plasmon Reson. Spectrosc. Gold Nanoparticle-Coat. Substrates. 19, 1–3.

[14] C. L. X. Liang, Z. Wang, (2010) Nanoscale Res Lett. 5, 124–129.

[15] G. Jiang, L. Wang, and W. Chen, (2007) Mater. Lett. 61, 278–283.

[16] B. Wong, S. Yoda, and S. M. Howdle, (2007) J. Supercrit. Fluids. 42, 282–287.

[17] L. Balogh, R. Valluzzi, K. S. Laverdure, S. P. Gido, G. L. Hagnauer, and D. a Tomalia, (1999) J. Nanoparticle Res. 1, 353–368.

[18] C. K. Tagad, S. R. Dugasani, R. Aiyer, S. Park, A. Kulkarni, and S. Sabharwal, (2013) Sensors Actuators B Chem. 183, 144–149.

[19] R. S. Patil, M. R. Kokate, C. L. Jambhale, S. M. Pawar, S. H. Han, and S. S. Kolekar, (2012) Adv. Nat. Sci. Nanosci. Nanotechnol. 3, 13-15.

[20] M. M. H. Khalil, E. H. Ismail, K. Z. El-Baghdady, and D. Mohamed, (2014) Arab. J. Chem. 7, 1131–1139.

[21] A. Biswas, S. Roy, and A. Banerjee, (2014) Zeitschrift für Anorg. und Allg. Chemie. 640, 1205–1211.

[22] W. H. Eisa and a. a. Shabaka, (2013) React. Funct. Polym. 73, 1510–1516.

[23] M. V. U. Kreibig, (1995) Springer-Verlag. 8, 142-178.

[24] B. Rodríguez-González, A. Burrows, M. Watanabe, C. J. Kiely, and L. M. Liz Marzán, (2005) J. Mater. Chem. 15, 1755.

[25] H. N. Verma, P. Singh, and R. M. Chavan, (2014) Vet. World. 7, 72–77.

[26] A. M. Abdelghany, E. M. Abdelrazek, and D. S. Rashad, (2014) Spectrochim. Acta Part A Mol. Biomol. Spectrosc. 130, 302–308.

[27] E. M. Abdelrazek, I. S. Elashmawi, a. El-khodary, and a. Yassin, (2010) Curr. Appl. Phys. 10, 607–613.

[28] L. H. S. Gasparotto, J. F. Gomes, and G. Tremiliosi-Filho, (2011) J. Electroanal. Chem. 663, 48–51.

[29] S. Sethia and E. Squillante, (2004) Int. J. Pharm. 272, 1–10.

[30] B. Singh and L. Pal, (2011) Int. J. Biol. Macromol. 48, 501–510.

[31] E. M. Abdelrazek, I. S. Elashmawi, and S. Labeeb, (2010) Phys. B Condens. Matter. 405, 2021–2027.

[32] G. M. T. and S. G. Tomlin, (1976) J. Phys. D Appl. Phys. 9, 1639.

[33] D.S. Davis and T.S. Shalliday, (1960) Phys. Rev. 118, 1020.

[34] A. V. J. Tauc, R. Grigorovici, (1966) Status Solidi. 15, 627.

[35] K. P. S. P. N Gupta, (1996) Solid State Ionics. 88, 319–323.

[36] M. T. E. Saion, (2006) Ionics 12. 5, 53–56.